

The effect of parameters on the end buffer impact force history of the crane

T N Haas, P Mainçon, P E Dunaiski

An overarching investigation was conducted to provide engineers with guidelines for designing crane supporting structures. The focus of this study was to determine whether the identified parameters had an effect on the end buffer impact force history when the electric overhead travelling crane collides with the end stops of the supporting structure. Seven design codes which were reviewed do not consider the crane and its supporting structure as a coupled system. This simplification ignores some of the parameters which have a significant influence on the impact force, which could lead to the codified estimates being sometimes unconservative. During the experimental tests it was discovered that some of the parameters could not be accurately controlled and/or monitored. This led to the development of a finite element (FE) model of the full-scale experimental configuration which was used to conduct advanced simulations. The FE model considered the crane and the supporting structure as a coupled system, in which the parameters were individually varied to obtain its effect on the impact force history. The results showed that some of the individual parameters do have a significant effect on the impact force history.

INTRODUCTION

Electric overhead travelling cranes (cranes) are used predominantly in industrial buildings to move heavy or cumbersome equipment, sometimes under very demanding conditions. Cranes enhance the operational process in industrial buildings, thereby improving production and ultimately reducing the production cost of the manufactured item. Hoist loads in these environments range from inconsequential (less than half a ton) to several hundred tons. Therefore the members of the crane and the crane supporting structure must be designed to have sufficient strength and stiffness to prevent failure at ultimate limit state and to prevent excessive deflection and vibrations at serviceability limit state.

In order to prevent local or global failure of the crane supporting structure, the following forces must be accurately assessed:

- Horizontal longitudinal forces due to the acceleration and braking of the crane, and the crane colliding with the end stops of the supporting structure.
- Horizontal lateral forces due to skewing of the crane.
- Vertical wheel loads due to the loaded hoist being lifted.

The work reported in this paper focuses on determining the horizontal longitudinal forces when the crane collides with the end stops of the supporting structure. Previously, crane operators believed that it was good practice to run the crane into the end stops

for realignment. Although the practice continues, it is less frequent nowadays. The constant collision between the crane and the supporting structure weakens the connection at the end stops. It is thus important that the horizontal longitudinal force resulting from the collision must be resisted by the end stops of the supporting structure. Failure of the end stops will result in the disastrous consequence of the crane running off the crane rails, especially when heavy loads are being hoisted. The consequences are even more disastrous if the hoist load is molten steel, as happened recently in China, when a crane which lifted molten steel ran off the rails, causing the load to be spilt on the ground. Several workers were killed when they were engulfed by the molten steel.

Several codes of practice and guidelines for the design of crane supporting structures were reviewed, namely:

- South African Standard: SABS 0160, 1989 (as amended 1990)
- Manufacturers' guidelines: DEMAG
- Eurocode 1, Part 3, EN 1991
- South African National Standard: SANS 10160, Part 6
- Australian Standard: AS 1418.14, 2001
- Australian Standard: AS 1418.1, 1994
- Association of Steel and Iron Engineers' technical report, AISE No 13, 1997

All the above codes of practice and guidelines consider the collision between the crane and the supporting structure as an accidental condition. This implies that this

TECHNICAL PAPER

JOURNAL OF THE SOUTH AFRICAN INSTITUTE OF CIVIL ENGINEERING

Vol 54 No 1, April 2012, Pages 55–62, Paper 752-A



DR TREVOR HAAS (Pr Tech Eng) is a Senior Lecturer in Structural Engineering at the Stellenbosch University. He obtained the National Diploma (1991) and National Higher Diploma (1992) in Civil Engineering from the former Peninsula Technikon, now Cape Peninsula University of Technology. In 1999 he was awarded the MS in Civil Engineering from

Southern Illinois University at Carbondale, USA. In 2007 he was awarded a PhD from the University of Stellenbosch. His research interests include numerical (FEA) modelling of steel structures, retrofitting of existing structures, structural dynamics and engineering education. He is a member of the Engineering Council of South Africa's universities of technology accreditation team.

Contact details:

Stellenbosch University
Department of Civil Engineering
Private Bag X1
Matieland
7602
South Africa
T: +27 21 808 4438
E: trevor@sun.ac.za



DR PHILIPPE MAINÇON obtained his engineering degree from the Ecole Centrale de Paris (France) and his Dr Ing degree from the Norwegian University of Science and Technology (Norway). He has lectured numerical methods in structural engineering at the University of Stellenbosch (South Africa), and is currently working at Marintek (Norway) as

a Senior Scientist. His research interests include inverse finite element methods for the processing of measurement data, flexible pipelines and risers for offshore applications, and vortex induced vibrations.

Contact details:

MARINTEK
SINTEF Marine
Otto Nielsens veg 10
Trondheim
Norway
T: +47 73 59 5687
E: Philippe.Maincon@marintek.sintef.no



PROF PETER DUNAISKI (Pr Eng), who sadly passed away in September 2011, was Professor in Structural Engineering at the University of Stellenbosch. He obtained the HBEng (1974), the MEng (1984) and the PhD (1991) degrees from the same university. His research interests were experimental mechanics and steel construction, with a focus on design aspects of commercial

and industrial structures. At the time of the preparation of this paper, he was also involved in code development for the South African structural engineering practice.

Keywords: crane, end buffer force, FE

Table 1 Parameters of the design codes used to estimate the end buffer impact forces

Code / Guideline	Impact speed	Impact speed reduction factor	Crane and crab mass	Payload mass	Dynamic factor to account for dynamic effects	Vertical position of the payload during impact	Horizontal position of the payload during impact	Damping characteristics (energy absorption of end buffers)	Longitudinal misalignment of the end stops	Power off (minimum load during impact)	Power on (maximum load during impact)
SABS 0160-1989											
Method (a) & Method (b)	×	×	√	×	×	×	×	×	×	√	×
DEMAG	√	×	√	×	×	×	×	√	×	√	×
EN 1991:3 & SANS 10160-6	√	√	√	√	√	×	×	√	×	√	×
AS 1418.18 : 2001	√	×	√	×	×	×	×	√	×	√	×
AS 1418.1 : 1994	√	√	√	×	×	×	×	√	×	√	×
AISE No 13: 1997	√	×	√	×	×	×	×	√	×	√	×



Figure 1 A view of the experimental model configuration

condition is seldom expected to occur during the life of the crane supporting structure. These codes estimate the end buffer impact force using a decoupled approach. This approach reduces the complexity of determining the member forces in the crane supporting structure. The codes consider several parameters that are used to estimate the end buffer impact force, as shown in Table 1.

Table 1 shows the parameters which the design codes explicitly use to estimate the end buffer impact force. It is evident that the design codes predominantly use the impact velocity, the mass of the crane and the end buffer's resilience to estimate the end buffer impact force. Other critical parameters which are omitted from the code specifications and guidelines are:

- i. The mass of the hoist load and its vertical and horizontal positions at the moment of impact.
- ii. The dynamic effects of the crane during impact.
- iii. The longitudinal misalignment of one of the end stops.
- iv. The effect of continuously running longitudinal motors during impact.

From Table 1 it is clear that the design codes do not consider the effect of all the critical parameters to estimate the end buffer impact force, and therefore, by ignoring these critical

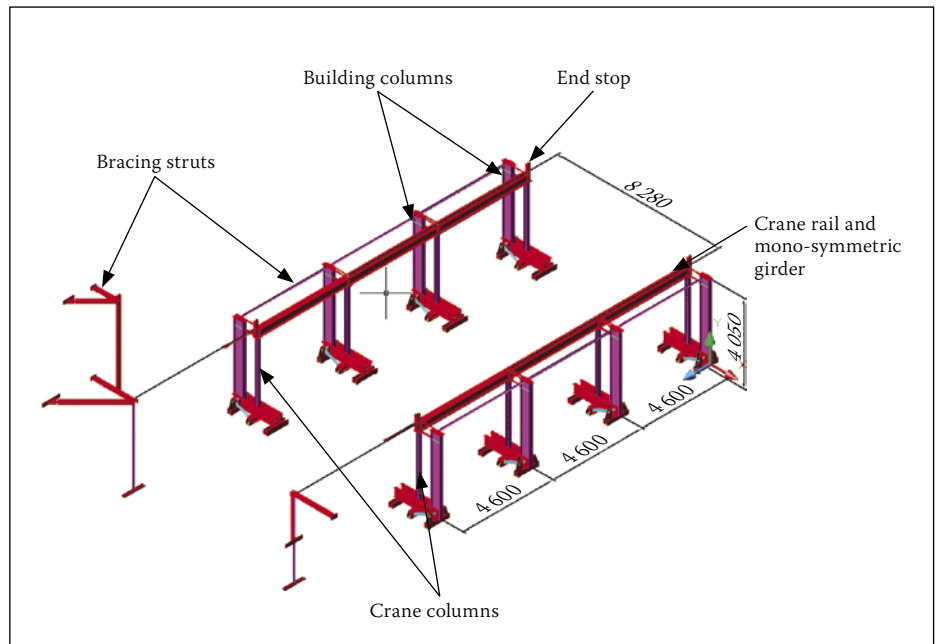


Figure 2 Numerical layout of the crane supporting structure

parameters, the design codes can substantially underestimate or overestimate the end buffer impact force. This study investigated which of the parameters listed in Table 1 had an effect on the end buffer impact force history. This information made it possible to determine whether the parameters should be included in a codified assessment of the end buffer impact force.

Besides the codes of practice, no other literature was found which directly relates to either experimental or numerical evaluation of end buffer impact forces.

This paper describes the experimental configuration, the codified end buffer impact force estimates, FE modelling of the crane and the supporting structure, and experimental and FE impact force history responses. Reasons for the discrepancies between the experimental and FE impact force history results are given. The paper ends with a summary and conclusions.

DESCRIPTION OF THE EXPERIMENTAL CONFIGURATION

Figure 1 shows the full-scale experimental configuration of the 5-ton electric overhead travelling crane and the supporting structure.

A brief description of the experimental configuration with reference to Figure 1 is now presented. The crane consists of a 305 × 305 × 118 H-section crane bridge which is 8.485 m long and two 203 × 203 × 60 H-section end carriages which are 4.140 m long with a lifting capacity of 5 tons (yellow structure). The hoist load consists of an in-fill lead concrete block which has a mass of 5.128 kg. DPZ 100 elastomeric cellular plastic buffers manufactured by DEMAG, are attached to the ends of the end carriages to absorb the impact during the collision (black sections at the ends of the end carriages). The elastomeric cellular buffer has an energy absorption capacity of 800 Nm with a corresponding deformation of 73 mm and a final end buffer impact force of

36 kN for an impact speed of 2 m/s as specified by the manufacturer. The crane supporting structure consists of $152 \times 152 \times 23$ H-section crane columns and $457 \times 191 \times 67$ I-section building columns which are 3.555 m long and spaced 4.596 m apart. Mounted on the crane columns is a mono-symmetric, simply supported steel girder which consists of a top flange (300×16 mm), a bottom flange (250×10 mm) and a web (350×20 mm), a 30 kg/m continuous railway rail and a continuous elastomeric pad sandwiched between the preceding members. The remaining members are equal angle sections used as bracing struts. Figure 2 shows the dimensioned drawing of the crane supporting structure with annotations.

DETERMINATION OF THE CODIFIED END BUFFER IMPACT FORCES

The codified end buffer impact forces were determined using the full-scale experimental crane configuration parameters described earlier. In Figure 3 the codified end buffer impact forces are presented as a function of the impact velocity of the crane.

From Figure 3 it is clear that there is a large discrepancy between the codified end buffer forces, which led to the conclusion that the codified estimates are not properly understood. This is due to the different analysis philosophies and parameters considered by the various design codes of practice. As a result of this discrepancy, an investigation was conducted to determine which parameters contribute significantly to the end buffer impact force.

METHODS

Experimental and FE Models

An experimental investigation was conducted to gain a better understanding of how the force resulting from the hoist load is transferred from the crane to the supporting structure. During the initial experimental investigations it was difficult to accurately control and measure the physical parameters, i.e. the pendulum action of the hoist load during acceleration and the constant velocity phases, misalignment of the end stops, the flexibility of the structure, the differential power output from the motor to the wheels and the differences in responses of the end buffers during impact. This difficulty can be attributed to the complex phenomena involved during the collision between the crane and the end stops of the supporting structure. A finite element (FE) model was therefore developed which considered the crane and supporting structure as a coupled system. The advantage of the FE

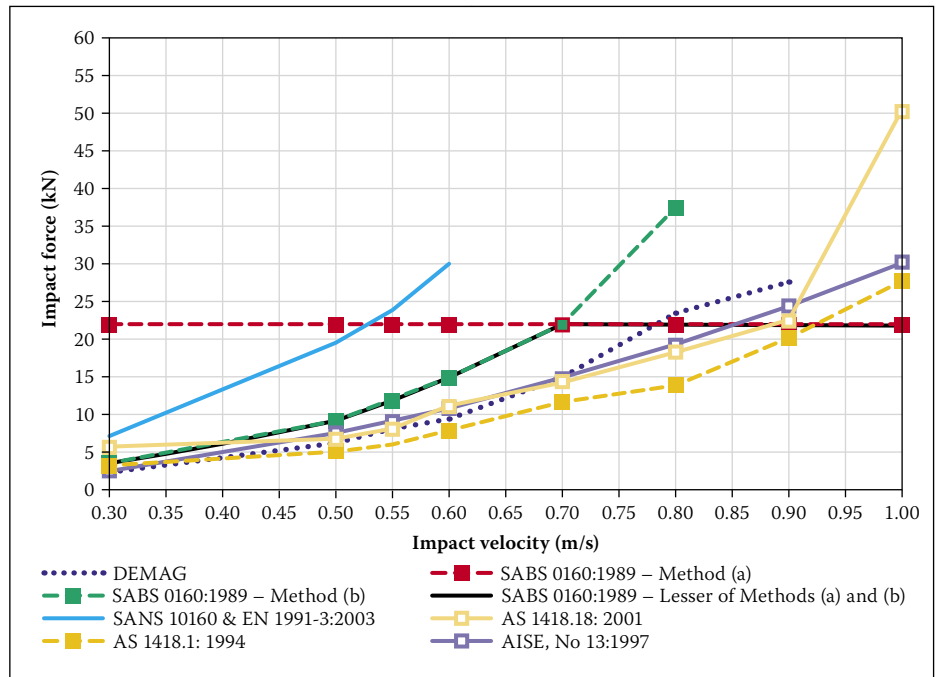


Figure 3 Graphical representation of the codified end buffer impact forces as a function of the impact velocity using a DPZ 100 cellular plastic buffer (energy absorber)

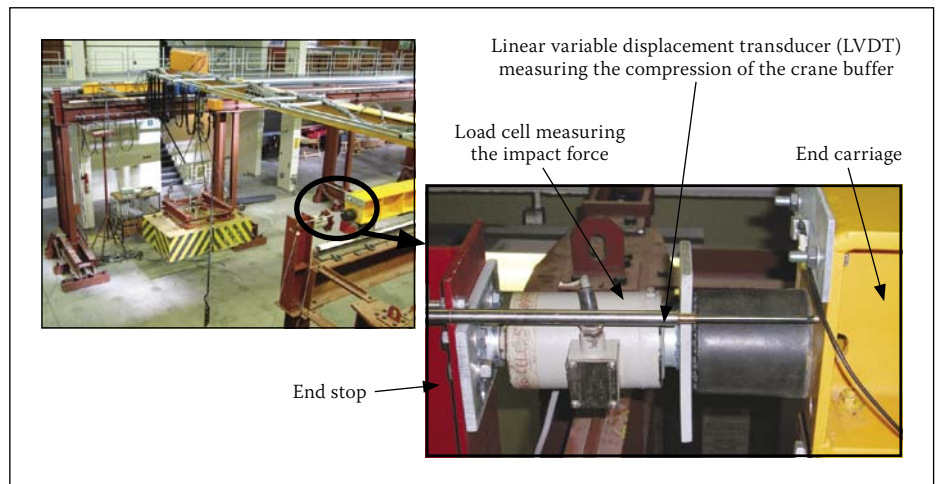


Figure 4 Experimental configuration of the crane buffer between the end carriage, the end stop and the load cell

model was that the parameters could easily be individually adjusted and controlled. Also, the entire experimental configuration was modelled to allow the other load models to be studied, i.e. vertical wheel loads and horizontal lateral loads.

Figure 4 places the measuring equipment of the experimental set-up in context in relation to the entire configuration. The measuring equipment was used to determine the impact force and displacement histories when the crane collided with the end stops.

Figure 4 shows the linear variable displacement transducer used to measure the compression of the buffer with a range of 100 mm and a resolution of $6.25 \mu\text{m}$, the load cell used to measure the compression force induced by the crane on the end stops with a capacity of 50 kN with a resolution of 3N, DEMAG's DPZ 100 end buffers which absorbed the energy during impact, and the

end stops which prevented the crane from running off the rails.

FE Model

Due to the complexity of the 5-ton crane and the supporting structure, many simplifications were required to obtain a computationally efficient FE model, i.e. an FE model that can conduct the simulations in the shortest possible time. A computationally efficient model was developed that properly captured the relevant physical system. Commercially available FE analysis software, ABAQUS version 6.5.4, manufactured by Dassault Systemes, was used to develop the FE model.

The purpose of the FE model was to generate accurate global forces and deflections of the members, as well as the contact forces between the various members of the coupled system. Since the stresses and strains

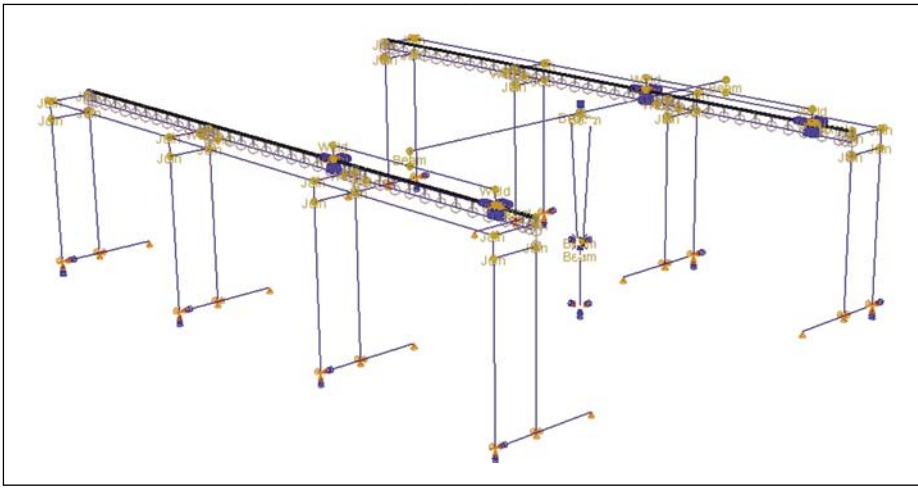


Figure 5 Schematic view of the FE model

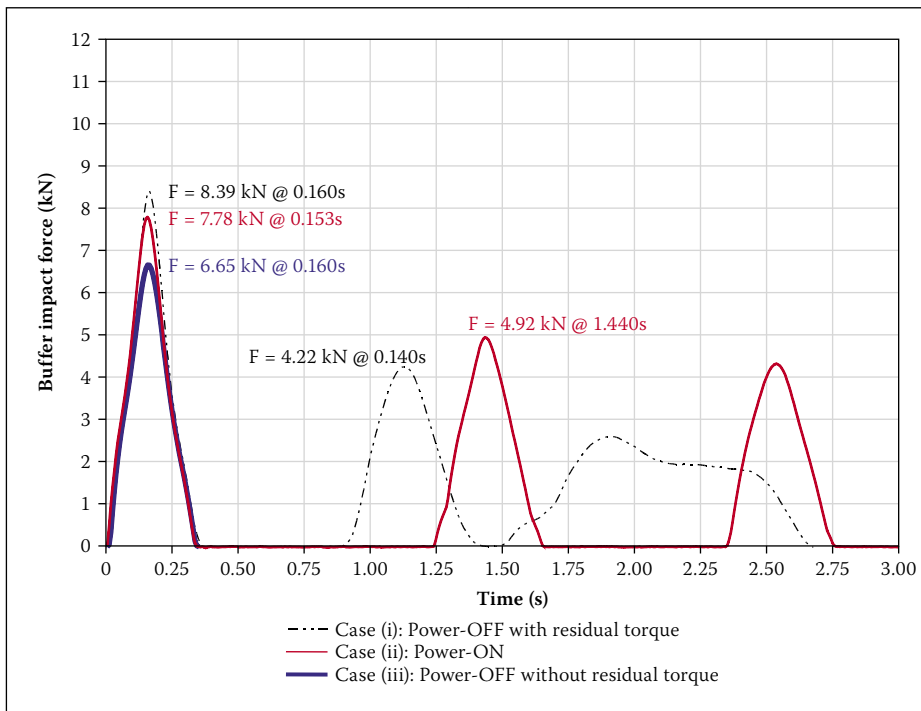


Figure 6 Comparison of the experimental end buffer impact force histories for case (i): “Power-Off with residual torque”, case (ii): “Power-On” and case (iii): “Power-Off without residual torque”

within the members were not of interest, the FE model consisted predominantly of three-dimensional shear flexible (Timoshenko) quadratic beam elements which were used to model the columns and beams. If the stresses and strains within the elements were required, it could be obtained using a detailed FE model of a specific element which consists mainly of solid (brick) elements using the global forces computed from the computationally efficient model. Spring elements with appropriate elastic and damping characteristics were used to model the highly non-linear DEMAG DPZ 100 cellular plastic buffers. Correctly defined contact properties were required for the interactions between the crane wheels and crane rails, as well as for the cable and pulley. A contact formulation was used that modelled near zero wheel friction in the longitudinal direction (rolling direction), with a non-zero wheel friction in the transverse

direction. The purpose of this paper was to describe the effect of the parameters on the impact force history of the crane, and thus a detailed description of the FE model is not presented. However, the reader is referred to Haas (2010) for a detailed description of the modelling techniques used to obtain a computationally efficient FE model. The simplifications resulted in an FE model which had 1 642 elements and 3 391 nodes with approximately 20 350 degrees of freedom (DOF). The average analysis time, including hoisting, acceleration and impact steps, was approximately 20 minutes on a Pentium 4 desktop computer with 3 GB of RAM. Figure 5 shows a schematic view of the FE model.

Description of the experimental tests and FE simulations

Experimental tests and FE simulations were conducted to determine the histories of the

end buffer impact force for the following hoist load conditions:

1. No hoist load.
2. Hoist load raised to 0.15 m above ground level (the minimum distance the hoist load could be lifted to clear any obstructions on the floor).
3. Hoist load raised to 2.20 m above ground level (the maximum distance the hoist load could be lifted).

For each of the three conditions, the hoist load was lifted to its respective height except for the condition of “No hoist load” before any tests were conducted. Once the hoist load and crane were free of any vertical vibrations, the crane was accelerated at 0.2 m/s^2 for 2.75 s to attain an impact velocity of 0.55 m/s. At the moment of impact the operator released the longitudinal acceleration button on the control pendant which allowed impact to occur as a result of the inertia of the crane and hoist load.

Experimental Impact Force

Condition: No hoist load

A proper understanding of the experimental impact force history was necessary before any calibration of the FE model could be done. Figure 6 shows the impact force histories for three different cases when the crane collided with the end stops without a hoist load, namely:

- i. “Power-Off with residual torque”: For this case, the acceleration of the longitudinal motors of the crane was disengaged at the moment of impact. Most modern cranes have a step-down/step-up torque function which controls the torque transmitted to the longitudinal motors, thus preventing the crane from stopping immediately when the longitudinal acceleration is disengaged. For this case, the torque was transmitted in a decreasingly linear fashion to the wheels of the crane when the acceleration button on the pendant was released.
- ii. “Power-On”: For this case, the acceleration of the longitudinal motors of the crane was engaged throughout the impact phase.
- iii. “Power-Off without residual torque”: For this case, the acceleration of the longitudinal motors of the crane, as well as the torque step-down function, was disengaged at the moment of impact, i.e. no power was transmitted to the wheels on impact.

The impact force history is also affected by the disc brakes of the wheels which engage the moment the operator releases the longitudinal acceleration crane motor button. The disc brakes were also disengaged for all cases during the experimental and FE tests. At least three tests were conducted for each

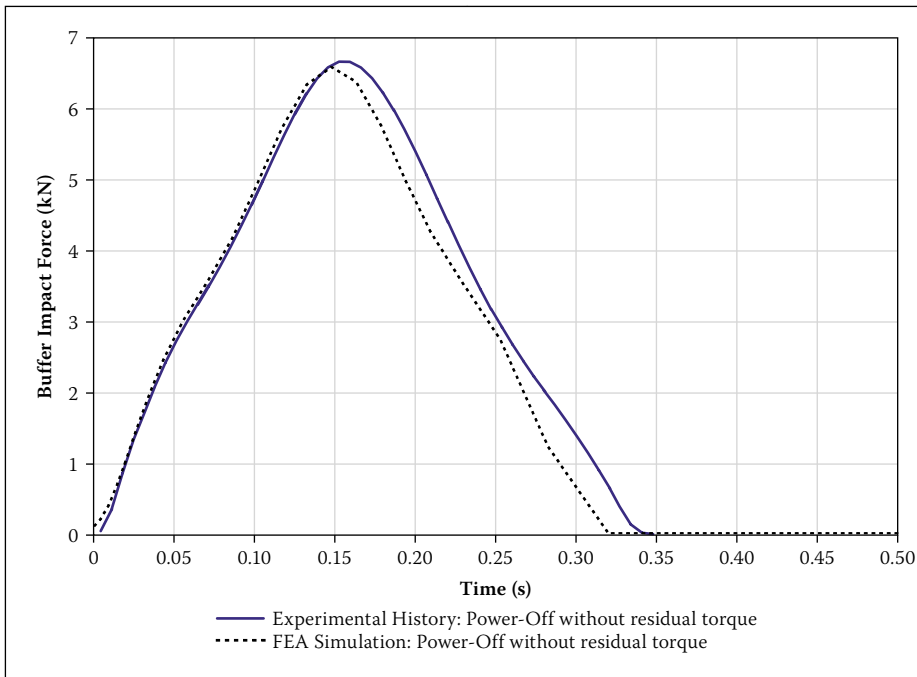


Figure 7 Comparison of the FE and experimental end buffer impact force histories without hoist load for "Power-Off without residual torque"

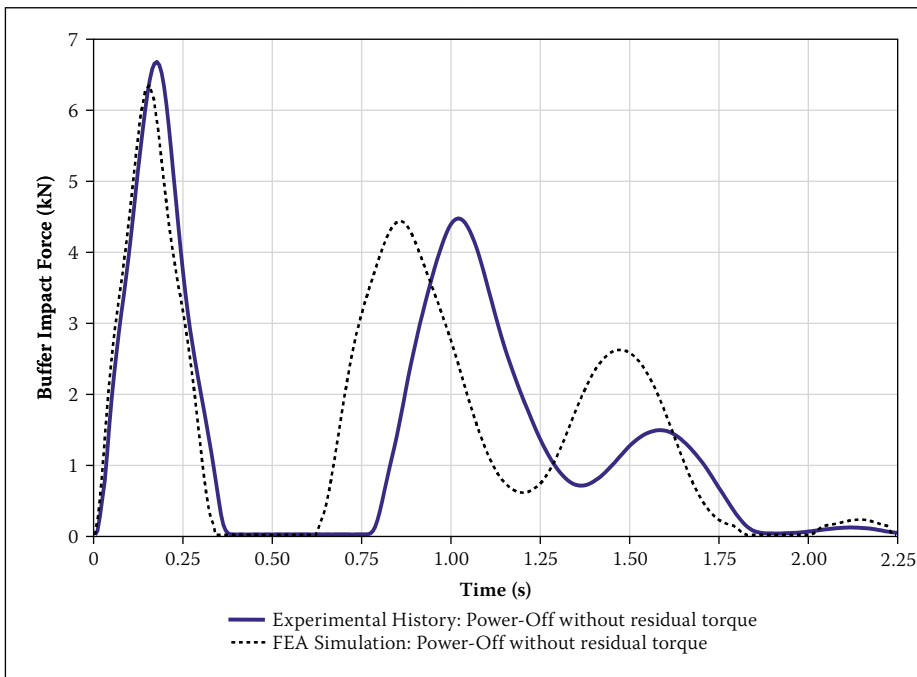


Figure 8 Comparison of the FE and experimental end buffer impact force histories with hoist load hoisted 0.15 m above ground level for "Power-Off without residual torque"

case. Thus the impact force histories shown in Figure 6 represent a series of experimental tests that were conducted to obtain the end buffer impact force histories for the three cases. All the other experimental results presented represent a series of tests conducted per case.

The expected end buffer impact force history for each case is shown in Figure 6 and is discussed individually.

Case (i) "Power-Off with residual torque"

Only one impact was expected when the crane without the hoist load collided with the end stops. Figure 6 shows two additional

peaks which occurred after the first impact. The secondary peaks are due to the variably adjusted step-down torque present in the longitudinal drive motors of the crane on impact, which propelled the crane back into the end stops.

Case (ii) "Power-On"

To determine the effect of the residual torque on the impact force history, a second series of tests were conducted when the crane collided with the end stops with the longitudinal drive motors fully engaged over a period of time. Figure 6 shows a comparison of the experimental tests for the "Power-Off with

residual torque" and "Power-On" conditions. The difference between the magnitudes of the first peaks is 7.8%, while the magnitudes of the second peaks differ by 16.6%. The time difference between the first peaks is insignificant, whereas the time difference between the second peaks was 26.3%. Therefore the residual torque had a significant influence on the impact force history.

Case (iii) "Power-Off without residual torque"

A third set of experimental tests was conducted by disengaging the residual torque to eliminate its effect on the impact force history. As expected, only one impact occurred since there was no residual torque to drive the crane back into the end stops. The first impact force was reduced by 20.7% when compared to the corresponding peak of case (i): "Power-Off with residual torque".

All further experimental tests were performed using case (iii): "Power-Off without residual torque", since this case yielded the expected impact force history, i.e. only one impact peak during the collision between the crane and the end stops of the crane supporting structure.

RESULTS

Calibration of the FE model to the experimental impact force history (no hoist load)

Figure 7 shows the end buffer impact force history of test case (iii) with the time reduced to 0.5 s. The FE simulations were conducted in the same way as for the experimental tests. When the original damping characteristics were used in the FE model, it resulted in a slight discrepancy in the impact force histories between the experimental and FE results. An improved FE impact force history was obtained by adjusting the buffer's damping characteristics by less than 5%. Superimposed on Figure 7 is the FE end buffer impact force history. The impact forces and occurrence of the peaks varied by less than 3%, proving that a good correlation was achieved between the experimental and FE impact force histories.

Comparison of the experimental and FE impact force histories

Condition: Hoist load raised 0.15 m above ground level

Except for the addition of the hoist load, the same experimental and FE models were used as for the condition "No hoist load" to obtain the impact force histories when the hoist load was lifted 0.15 m above ground level.

The hoist load was symmetrically positioned on the crane bridge and lifted 0.15 m above ground level for both the experimental tests and the FE simulations. Figure 8 shows the superimposed experimental and FE impact force histories for this case.

From the experimental tests it was observed that, after the first impact, the buffers lost contact with the end stops for 0.42 s before impacting the end stops for two consecutive collisions. The second and third impacts were due to the hoist load's inertia during its pendulum motion as the hoist load yanked the crane into the end stops. The secondary impacts occurred as expected. The experimental history resulted in three impacts which occurred at 0.17 s, 1.02 s and 1.69 s with magnitudes of 6.68 kN, 4.47 kN and 1.48 kN respectively.

The FE simulations followed the same trend as the experimental history, but with some discrepancies. The FE simulations resulted in three impacts which occurred at 0.15 s, 0.88 s and 1.48 s with magnitudes of 6.35 kN, 4.43 kN and 2.61 kN respectively.

The differences in the magnitudes of the first and second impact peaks between the experimental and FE histories were 4.9% and 0.9%, while the differences in time were 11.7% and 13.7% respectively. A negative shift of 0.14 s occurred between the second peaks of the experimental test and the FE simulation. The reasons for the discrepancies were not obvious and required further investigation. Additional impact tests were conducted with the hoist load raised to 2.20 m above ground level to determine the differences between the experimental and FE impact histories.

Condition: Hoist load raised 2.20 m above ground level

The hoist load was raised to 2.20 m above ground level, instead of 0.15 m as in the previous case. Figure 9 shows the superimposed experimental and FE impact force histories for this case.

In the experimental impact tests, the buffers did not lose contact with the end stops for the entire duration of the tests. The experimental histories resulted in three impacts which occurred at 0.16 s, 0.73 s and 1.04 s with magnitudes of 7.08 kN, 2.74 kN and 3.89 kN respectively. Surprisingly, the second impact was smaller than the third impact. A possible reason for this is the cancellation of various modes during impact.

The FE simulation predicted the first impact reasonably accurately, but thereafter the FE simulation results deviated substantially from the experimental test history. The numerical impacts occurred at 0.16s, 0.75 s and 1.30 s with magnitudes of 6.59 kN,

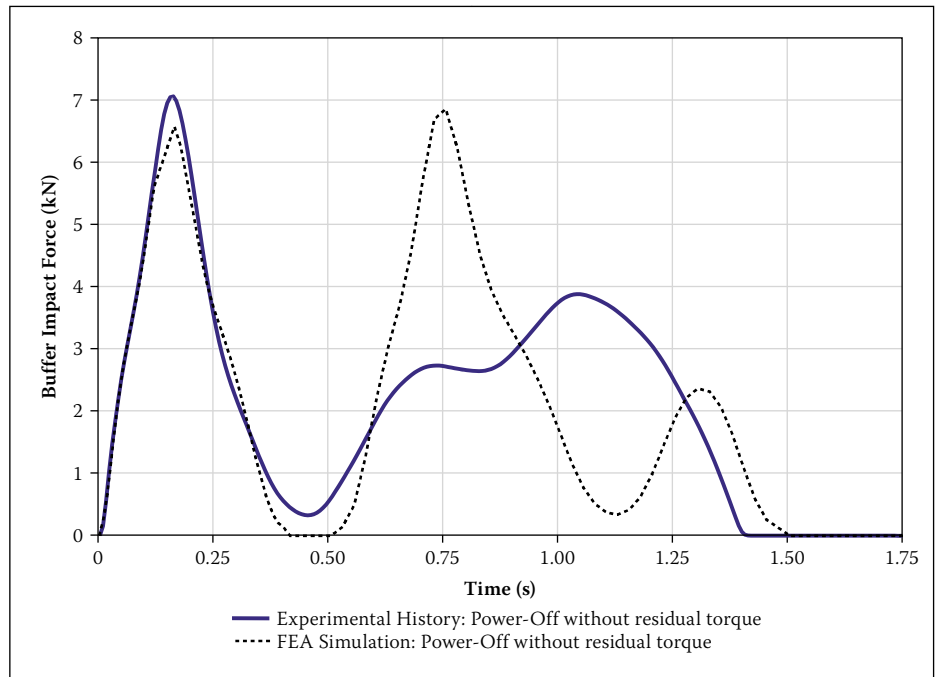


Figure 9 Comparison of the FE and experimental end buffer impact force histories with hoist load hoisted 2.20 m above ground level for "Power-Off without residual torque"

Table 2 Comparison of the FE and experimental parameters discrepancies

Parameters	Experimental Configuration	FE Configuration
Horizontal hoist load lag with respect to the crane bridge at the moment of impact	Not measured (difficult to measure)	Known lag angle = 0° Can be varied or kept constant
Crab position on the crane bridge	At midspan	At midspan
End stop misalignment in relation to each other	No measurable misalignment	No misalignment
Crane supporting structure's flexibility during impact	Not measured	Known from FE simulations Exact
Crane velocity at the moment of impact	0.55 m/s ±	0.55 m/s Exact
Elastic characteristics of buffer	Similar up to 5 kN at 35 mm compression, then differs significantly	Identical for both buffers
Damping characteristics of buffer	Slight discrepancy in buffers	Identical for both buffers
Release of the longitudinal acceleration button at the moment of impact	Done by operator, can vary significantly Not exact	Released at the moment of impact Exact

6.88 kN and 2.37 kN respectively. In the FE simulations the buffers lost contact with the end stops for 0.12 s after the first impact.

DISCUSSION

Possible reasons for the discrepancies between the experimental and FE impact force histories

After careful observation of the video footage of the experimental tests and the FE simulations of the impact force histories, it was discovered that certain parameters had a significant influence on the end buffer

impact force history. A slight change in the magnitude of the parameters can lead to significantly different impact force histories. Table 2 lists the parameters which were identified as having a significant influence on the end buffer impact force history, and gives a comparison of the discrepancies between the FE and the experimental test parameters.

The discrepancies between the parameters of the experimental tests and the FE models led to the surmise that this could be the reason(s) for the differences in the impact force histories when the hoist load is included in the analysis. FE simulations were

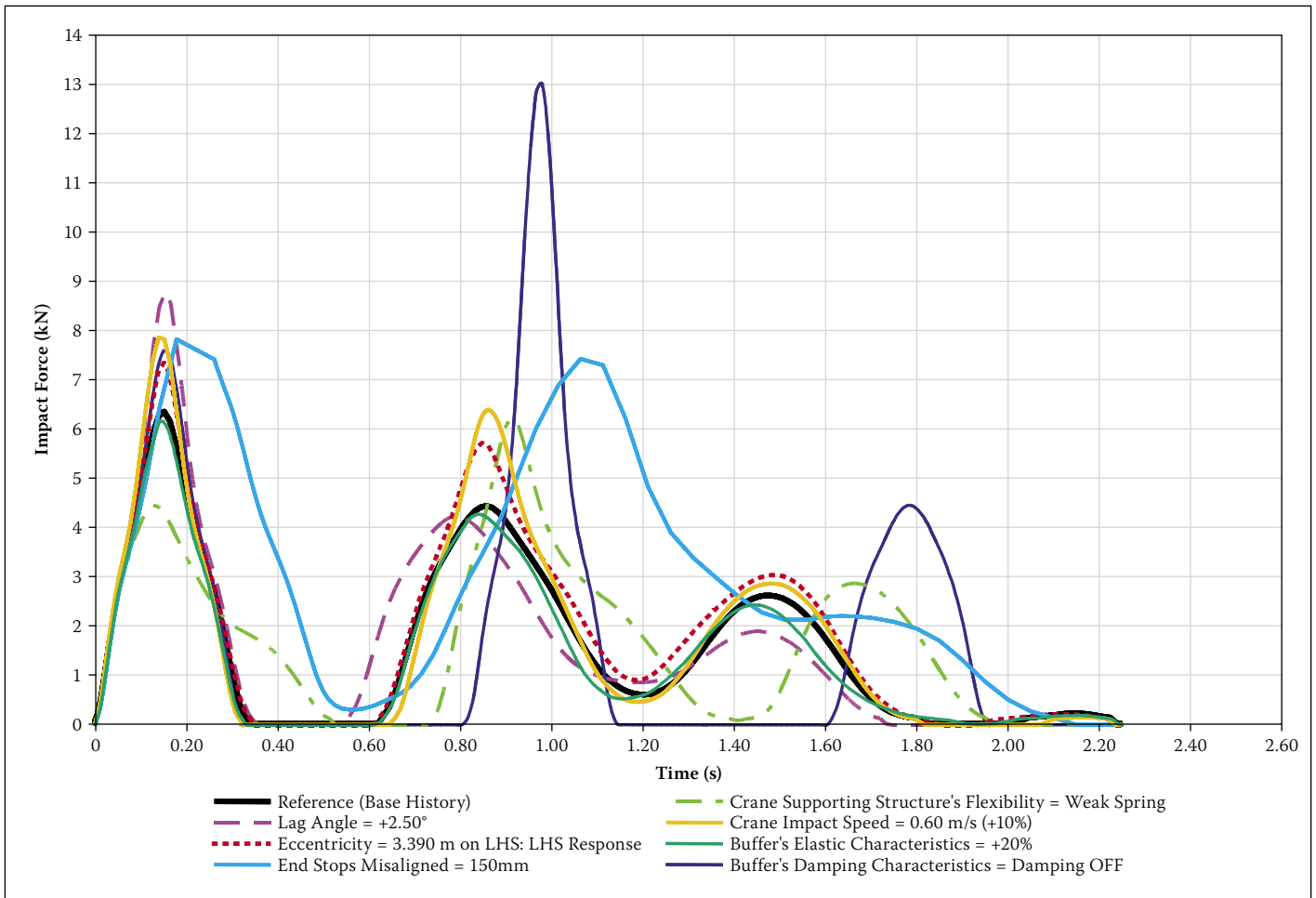


Figure 10 Impact force history of each parameter compared to the base history with hoist load hoisted 0.15 m above ground level

conducted using the parameters identified in Table 2, together with carefully chosen parameter variations which were observed in the experimental and FE simulations. The initial investigation was conducted by individually varying parameters in the FE model. Figure 10 shows arbitrarily selected impact force histories obtained when the magnitude of a single parameter was varied at a time with the remaining parameters kept constant.

Figure 10 shows the large variation in the first and second impact force peaks and the position of the peaks when the individual parameters are varied. This indicates that a change in the magnitude of the parameters does indeed have a significant influence on the impact force histories, suggesting that the differences between the experimental and FE impact force histories can be attributed to the contribution of the individual parameters when the hoist load is lifted. The range of variation of the parameters in the study was based on the parameter variability which was obtained from observation of the experimental and video footage. A detailed list of parameter variations is given in the paper following on this one, i.e. paper 752-B on page 63, titled *Estimation of the maximum end buffer impact force for a given level of reliability*.

SUMMARY AND CONCLUSIONS

The FE impact force histories show that, by adjusting the magnitude of the parameters individually, the impact force histories are significantly affected compared to the base impact force history. An improved match between the experimental and FE histories with the hoist load attached could be achieved through extensive parameter fitting of the FE model. This was abandoned as irrelevant since the magnitudes of the parameters obtained for the improved match would be for a particular situation only, e.g. the magnitudes of the parameters would differ when the position of the hoist load was altered.

The codes of practice for the design of structures yield very different results, as different analysis philosophies and factors are taken into account for the estimation of the end buffer impact force. These approaches are based on a decoupled analysis of the crane and the crane supporting structure. This results in important parameters being omitted in the estimation of the end buffer impact forces, which can lead to substantially under- or overestimated end buffer impact forces.

Although the particular combinations of the parameters and their magnitudes which caused the discrepancies between the FE and experimental histories were not found, it is

believed that the sensitivity to the identified parameters (mechanisms) indicate that there is significant room for error in the codified end buffer impact forces.

Evidence was provided that the parameters omitted by the codes of practice do indeed have a significant influence on the end buffer impact force history. Crane failures could easily occur if these parameters are not properly accounted for. The effect of varying the magnitudes of the parameters in the FE simulations was investigated in detail through a sensitivity study and is presented in the paper following on this one, i.e. paper 752-B on page 63, titled *Estimation of the maximum end buffer impact force for a given level of reliability*.

BIBLIOGRAPHY

- ABAQUS, Personal communication and www.abaqus.com
- Association of Steel and Iron Engineers (AISE) 2000. *Specification for electric overhead travelling cranes for steel mill service*, Technical Report 6, Clause 3.8, pp 48–49.
- DEMAG. Cranes and components, buffers. DPZ 100 cellular plastic buffers, DPG rubber buffers, DPH hydraulic buffers.
- European Committee for Standardisation 1991. EN 1991-3:2003, EUROCODE 1 – *Actions on structures*,

Part 3: Actions induced by cranes and machinery, CEN/TC250/SC1, Clause 2.11.1, pp 1–44.

Haas, T N, Mainçon, P & Dunaiski, P 2010. *Finite element analysis modelling of full scale 5-ton electric, overhead travelling crane and the crane supporting structure*. Paper presented at the 4th International Conference on Structural Engineering, Mechanics and Computation, University of Cape Town, South Africa, 6–8 September 2010.

South African Bureau of Standards. 1989. SABS 0160-1989 (as amended 1990): *Code of practice for the general procedure and loadings to be applied in the design of buildings*. Clauses 5.7.6 and 5.7.7, pp 95–100.

South African Bureau of Standards. SANS 10160-6: Working document on SANS 10160: *Basis of structural design and actions for buildings and industrial structures, Section 10: Action induced by cranes and*

machinery. Personal communication with a Member of the Working Group, Clause 10.2.12.1, pp 1–26.

Standards Australia. 1994. AS 1418.1:1994: *Cranes (including hoists and winches). Part 1: General requirements*, 3rd edition. Clause 4.7.5, pp 24–26.

Standards Australia. 2001. AS 1418.18:2001: *Cranes (including hoists and winches). Part 18: Crane runways and monorails*. Appendix B, p 41.